

Progressive shortening of sp-hybridized carbon chains through oxygen-induced cleavage

Gianpietro Moras,^{*,†,‡} Lars Pastewka,^{†,¶} Michael Walter,[§] Johann Schnagl,^{||} Peter Gumbsch,^{†,‡} and Michael Moseler^{†,§}

Fraunhofer Institute for Mechanics of Materials IWM, 79108 Freiburg, Germany, Karlsruhe Institute of Technology, Institute of Applied Materials - Reliability of Components and Systems IAM-ZBS, 76131 Karlsruhe, Germany, Johns Hopkins University, Department of Physics and Astronomy, Baltimore, MD 21218, USA, University of Freiburg, Institute of Physics, 79104 Freiburg, Germany, and BMW Group, 80788 München, Germany

E-mail: gianpietro.moras@iwm.fraunhofer.de

*To whom correspondence should be addressed

†Fraunhofer Institute for Mechanics of Materials IWM

‡Karlsruhe Institute of Technology

¶Johns Hopkins University

§University of Freiburg

||BMW Group

Abstract

Linear sp -hybridized carbon chains have recently been proposed as one-dimensional nanostructures for electronic applications, and as intermediate products in many nanoscale processes. However, their synthesis and observation is affected by their degradation upon oxygen exposure. Carbon chains consisting of alternating single and triple bonds (polyyinic) are reported to be more stable than those consisting of double bonds (cumulenic), but the details of the degradation mechanism are still unknown. We use density functional theory to show that adsorption of O_2 on carbon chains anchored to carbon substrates can cause their cleavage through the collective scission of O–O and C–C bonds, yielding separate CO-terminated chains. Further O_2 attack progressively shortens them causing CO_2 formation. While the shortening process has general validity, the cleavage step of the reaction is exothermic for cumulenic chains only. Perturbations of the ideal structure, such as bending of the chains or modifications to the structure of their termination, affect the oxidation mechanism and can make the cleavage reaction exothermic for polyyinic chains as well. These results contribute to the interpretation of the available experimental results and reveal atomic-scale details of the oxidation process, thus allowing predictions on the chemistry of nanostructured carbon surfaces and suggesting possible new directions for the study of the chemical stability of carbynoid structures.

Keywords: carbynoid nanostructures, carbon allotropes, oxidation, density functional theory

Introduction

Alongside the sp^2 - and sp^3 -hybridized allotropes, a one-dimensional sp -hybridised form of carbon^{1–3} is currently receiving increasing attention for its potential electronic applications^{4–6} and its precursor role in many nanoscale processes. For example, carbon chains have been observed or hypothesized to form during the transmission electron microscopy imaging of graphene,^{7,8} the preparation⁹ and fracture¹⁰ of carbon nanotubes, the formation of nanostructures in carbon plasmas,^{11,12} the growth of amorphous carbon films,^{13,14} and the mechanical polishing of diamond surfaces.¹⁵ Although the existence of *carbyne*, a solid entirely composed of sp -hybridized carbon,

has long been disputed,^{1,3} chemical^{16–21} and physical^{22–27} routes have been designed to obtain partially carbynoid structures.

It is not surprising that the main issue in both the synthesis and the observation of these structures is their extreme chemical reactivity.²⁸ Carbon chains in cluster-assembled carbon films²⁹ tend to undergo cross-linking to form a more stable sp^2 phase even in ultra high vacuum. Moreover, exposure to O_2 leads to their fast disappearance through chemical routes that have not yet been clarified. The degradation of carbynoid structures consisting of alternating single and triple bonds (*polyynes*¹⁹) is slower than that of chains consisting of double bonds (*cumulene*¹⁹), and a small fraction of the polyynic structures is reported to survive air exposure.²⁹ A detailed understanding of the underlying degradation mechanisms would aid the search for stabilization procedures during the chemical synthesis of carbyne-like structures. The latter often relies on end-capping groups or reaction byproducts that protect the chains from the contact with other chains and with air.^{29,30} Indeed, relatively long (up to 44 C atoms) polyynes that are stable in normal laboratory conditions²¹ were synthesized using complex, sterically large end-capping groups.^{17–21}

The degradation mechanisms that affect the synthesis of carbon chains can play a role in the material processes where their presence has been reported. For instance, some of us recently proposed that oxygen-induced degradation of carbon chains that form during mechanical polishing of diamond¹⁵ and wear of amorphous carbon³¹ contributes to the removal of carbon from the surfaces. Also, residues of the chemical reactions which degrade the carbon chains upon air exposure may determine the chemical termination of the underlying carbon substrate, *e.g.*, graphene⁸ or nanotube¹⁰ edges and carbon surfaces obtained by vapor deposition.^{13,14}

In this work, we use density functional theory (DFT) simulations to shed light on the mechanisms leading to the degradation of carbynoid structures in presence of O_2 . First, we demonstrate that the O_2 -induced cleavage reaction hypothesized by Sowa *et al.*³² in the case of cyclic carbon clusters in the gas phase is possible on energetic grounds. This lifts some inconsistencies in the original energetic estimates and establishes the viability of DFT for the systems under consideration. The reaction proceeds through the chemisorption of O_2 on cluster C–C units followed by the

concerted breaking of the O–O and C–C bonds, which cleaves the cyclic carbon chain.

Next, we investigate whether the same cleavage mechanism is possible for supported carbon chains. We find that this is energetically and kinetically viable for double C–C bonds of cumulenenic chains but it is not generally valid for polyynic structures, in agreement with experimental results.^{17–21,29} However, the mechanical and electronic properties of the carbynoid structures, and in turn the details of their oxidation, are influenced by the chains’ bending³³ and by the structure of their terminations.^{30,34,35} For instance, modifications to the relative orientation of the terminal groups of a cumulenenic chain or to the number of atoms composing a polyynic chain introduce perturbations to the ideal orientation of the π orbitals or to the triple/single bond alternation, respectively. We observe that bending strain facilitates the cleavage reaction, making the cleavage of triple bonds at polyynic structures possible. Perturbations of the ideal cumulenenic or polyynic bond structure, instead, do not seem to influence the energetics of such reactions. Bonds with π orbitals are still favorable sites for oxygen adsorption and, in some cases, for C–C bond cleavage.

Finally, we show that oxygen-terminated supported chain fragments resulting from the cleavage reaction, independently of the structure of their anchoring sites, undergo an oxygen-induced shortening process. The latter proceeds through the cleavage mechanism introduced above and the formation of CO₂. These atomic-scale details allow predictions about the chemical structure of carbon chains that survive oxygen exposure and about the chemical terminations of surface sites where degraded chains were anchored.

Methods

DFT calculations

The spin-polarized DFT calculations were performed using a grid-based real-space implementation of the projector augmented wave (PAW) method^{36,37} (as implemented in the GPAW code) and the PBE generalized gradient approximation³⁸ to the exchange and correlation functional. Additionally, a post-TPSS³⁹ correction to the PBE energies was used for the oxidation of cyclic carbon

clusters in the gas phase. This is able to improve the binding energy of the O₂ molecule (5.38 eV, where 5.23 eV is the experimental value) with respect to the overestimated 6.35 eV obtained with the PBE functional. All DFT calculations were performed using a 0.2 Å grid spacing and about 5 Å vacuum surrounding the clusters. A maximum force threshold of 0.025 eVÅ⁻¹ was used during the geometry optimization simulations using the fast inertial relaxation engine (FIRE) algorithm.⁴⁰ The charges were obtained by means of the Bader analysis.⁴¹

Calculations of the potential energy barriers

The potential energy barriers for the adsorption of O₂ to the cyclic cluster in the gas phase and for the shortening of the supported oxygen-terminated chains were performed through constrained geometry optimization simulations. In the former case, the distance between the O–O and C–C bond centers was constrained. In the latter case, we constrained the distance between the C atoms of the breaking C–C bond, or the C and O atoms involved in the formation of the second C–O bond between O₂ and the chain. In all other cases, the barriers were calculated through an improved tangent estimate in the nudged elastic band (NEB) method.⁴²

Reaction rate estimate

The estimation of the reaction rates for the OC₁₀O⁺ → OC₉⁺ + CO and OC₉⁺ → C₈⁺ + CO reactions were obtained using the RRKM transition state theory in the classical limit.⁴³ Within the latter, the reaction rate is expressed as

$$k(E) = \left(\frac{E - E_0}{E} \right)^{s-1} \frac{\prod_{i=1}^s \nu_i}{\prod_{i=1}^{s-1} \nu_i^\ddagger}, \quad (1)$$

where E is the energy available for the reaction (*i.e.* the total, kinetic plus potential energy of the unfragmented cluster, measured with respect to its minimum potential energy), E₀ is the energy barrier, s is the number of vibrational modes ν_i of the cluster, and ‡ indicates the vibrational

frequencies of the transition state. We calculated the vibrational modes using our DFT setup and used the post-TPSS-corrected values for E and E_0 . A lower bound estimate for the detachment rate of the second carbonyl group was made by assuming that the first CO fragment has zero kinetic energy.

Results and discussion

Gas phase cyclic clusters

Sowa *et al.*³² reported cross sections for the reaction of mass-selected carbon cluster cations with O_2 . In particular, in the case of C_n^+ clusters with $n \geq 8$, which are expected to be monocyclic,⁴⁴ this reaction yields almost exclusively C_{n-2}^+ as its detectable product at low collision energies. As a consequence, the authors propose an oxidation mechanism starting with the concerted addition of O_2 to a double bond of the C ring, with an activation barrier of a few tenths of eV. This should lead to the exothermic opening of the ring, causing the formation of a linear OC_nO^+ cluster with an estimated internal energy of about 4 eV plus the collision energy. In order to reach the final C_{n-2}^+ product, the linear OC_nO^+ must lose both CO terminal groups. However, each of these bond-breaking reactions is estimated to require about 4 eV and the available internal energy is therefore not sufficient for their detachment.³² The energy landscape for the proposed reactions is sketched in Figure 1 (black line).

In order to solve this inconsistency, we investigate this mechanism on the C_{10}^+ cyclic cluster through spin-polarized DFT calculations,³⁷ using the PBE generalized gradient approximation (GGA)³⁸ and the TPSS meta-GGA³⁹ exchange and correlation functionals. The barrier for the concerted addition of O_2 to a C–C bond of the carbon ring is determined through a series of constrained geometry optimizations for different, fixed values of the distance between the centers of the C–C and O–O bonds. To avoid spin-flipping during this procedure, we constrain the system to be in a doublet spin state. Indeed, the ground state of C_{10}^+ being a doublet state,⁴⁴ the adsorption reaction can occur on the doublet potential energy surface regardless of the spin state of the ad-

sorbing O₂ molecule,⁴⁵ therefore allowing for a possible triplet-to-singlet transition of the O₂ spin state.

Our calculations confirm that both the chemisorption of O₂ to a C–C bond and the subsequent breaking of the C–C bond are exothermic reactions with a negligible associated energy barrier. Crucially, using the PBE functional, the potential energy of the resulting OC_nO⁺ linear product is 8.57 eV lower than the energy of the reactants, *i.e.* more than two times the value proposed in Ref. 32. In agreement with the estimates in the latter, we find that the detachment of the first and second carbonyl groups requires 4.00 and 4.47 eV, respectively. Taking into account some collision energy, and the fact that there is no efficient way to dissipate the considerable internal energy of the OC_nO⁺ cluster in the dilute gas phase, this makes the loss of the two carbonyl end groups possible (Figure 1, red line). Furthermore, using a post-TPSS correction to the PBE energy,³⁹ which is able to correct the PBE overestimation of the O₂ cohesive energy (see Methods section), we find that the energy gain caused by the ring cleavage is even larger. This results in the C₈⁺ + 2 CO products being 0.99 eV lower in energy than the C₁₀⁺ + O₂ reactants (Figure 1, green line).

We estimate the time needed for the detachment of the two carbonyl groups using the RRKM transition state theory in the classical limit⁴³ (see Methods section). This yields a ~10 ps time for the detachment of the first carbonyl group and a lower bound of ~0.1 μs for the detachment of the second one. While these time-scales are too long for DFT-based molecular dynamics simulations, they are compatible with the experimental time-scales.

Supported carbon chains

A more effective way to dissipate the internal energy of the cluster after its cleavage, such as the coupling with a substrate, would probably prevent the terminal carbonyl groups to detach from the cleaved carbon chain. The cleavage process could however still occur through the same route described above. We investigate this possibility with the same DFT approach used in the gas phase, this time opening the carbon ring and anchoring the resulting linear cluster to a substrate. The presence of a substrate is modeled by terminating the carbon chain with hydrogen atoms and

fixing the positions of the terminal carbon and hydrogen atoms during the simulations. The validity of such a model is tested against adsorption results obtained on a periodic acene model substrate and is justified by the fact that the oxygen adsorption on the carbon chain depends locally on the chemical characteristics of the adsorption site, as explained below.

The geometrical and chemical properties of these linear chains depend on the structure of the anchoring sites on the substrate. The positions of the anchoring sites determine the curvature and the internal strain of the carbynoid structures. More importantly, the hybridization and orientation of the anchoring carbon atoms dictate the chemical structure and electronic properties of the chain.³⁴ For instance, a CH_2 -terminated carbon chain has a cumulenic character. A chain with CH_3 or phenyl terminations has a polyynic structure if it is even-numbered, while it has a “defective” structure, which deviates from the ideal cumulenic/polyynic classification, if it is odd-numbered. Moreover, the electronic properties of cumulenic chains are strongly influenced by the relative orientation of the terminal groups, since it determines the orientation of the staggered π orbitals.³⁴

To take this complex scenario into account, we investigate the viability of the oxygen-induced cleavage reaction presented above for the gas-phase clusters on the model systems depicted in Figure 2. We focus on C_8 supported clusters and then test the validity of our results for longer chains. Polycumulenic (Figure 2a) and polyynic (Figure 2b) straight chains are considered, where the positions of the atoms are relaxed before fixing those of the terminal carbon and hydrogen atoms. A qualitative representation of the differently oriented double bonds of a cumulenic chain and of the triple and single bonds forming a polyynic chain is provided by the Electron Localization Function (ELF)^{46,47} isosurfaces in Figure 2c,d. The cumulenic chain (Figure 2c) is characterized by a series of elongated bilobal isosurfaces, oriented as the π orbitals, *i.e.* each isosurface is rotated by 90° with respect to the adjacent ones. For the polyynic structure (Figure 2c) instead, the ELF isosurfaces have a cylindrical shape, centered on each bond. They are localized at the C–C bond center for single bonds, while delocalized towards the π orbitals at triple bonds. Perturbations of these structures are also taken into account. By rotating one of the two terminal CH_2 groups of the cumulene structure of Figure 2a by 90° (Figure 2e), an axial torsion and a modification

of the electronic structure are induced³⁴ (*e. g.* the spin state changes from singlet to triplet³⁵). The alternation of single and triple bonds of the polyyne chain of Figure 2b is not affected by torsional effects but is perturbed by adding one carbon atom to the chain instead (Figure 2f). The ELF isosurfaces for the perturbed systems are shown in Figure 2g,h. The effect of the curvature is studied for both cumulenic and polyyenic chains, and different curvatures are enforced by using two sets of positions for the fixed H atoms. The first set of H positions is obtained by optimizing the geometry of the chain and the terminal H atoms, while keeping the positions of the terminal C atoms fixed (Figure 2i). In the second, more strained, configuration (Figure 2j), we use the H positions provided by the geometry optimization of a cleaved chain, composed by two separated fragments. In both cases, the distance between the two fixed C atoms is chosen so that the chain can be placed on an acene model system used to investigate the role of a more realistic substrate (Figure 2k). In this case two hydrogen atoms are used to saturate the carbon dangling bonds below the chain in order to prevent the chain to link to the substrate. As a consequence C₁₀ is used instead of C₈, since the latter would be too strained by the presence of the two hydrogen atoms.

The DFT energies of the local potential energy minima relevant to the adsorption of O₂ on the supported systems of Figure 2 and their oxygen-induced cleavage are summarized in Figure 3. Here, the energy of the carbynoid structure with a non-adsorbed oxygen molecule in its ground state is taken as the reference zero energy for each investigated system (see the example in Figure 3a for a straight cumulenic chain, where the spin polarization density isosurfaces indicate a triplet spin state for O₂). It is important to note that, while the cleavage reaction can potentially occur as in the gas phase case (see Panels a-e in Figure 3) when O₂ adsorbs on C–C bonds of cumulenic chains and on triple bonds of polyyenic chains, the same reaction is not possible when single C–C bonds are “attacked” by O₂. In the latter case, upon O₂ adsorption we observe just one possible potential energy minimum configuration (Figure 3f), where the oxygen molecule splits, resulting in a new CO bond and an epoxide group. Firstly, this configuration cannot lead to the cleavage of the C–C single bond, since this would be an endothermic reaction. Secondly, the adsorption reaction is exothermic for bended chains only (by 1.14 eV), and the adsorption on the

adjacent triple C–C bonds would be in all cases energetically favorable (see Figure 3).

Oxygen chemisorption

We first analyze the results obtained for the adsorption of O₂ on cumulenic structures (black symbols in Figure 3). O₂ chemisorbs at C–C double bonds with the O₂-containing plane aligned with the π orbitals (see ELF isosurfaces in Figure 2c). A first local energy minimum configuration is depicted in Figure 3b: a C–O bond forms and the O–O bond length is stretched to 1.35 Å. This is a superoxo state, where one electron is donated by the carbon atoms to one of the two π^* orbitals of the O₂ molecules. This causes the O₂ spin state to change from triplet to doublet, while the total spin state of the system remains a triplet. The energy of this superoxo configuration is however higher than the energy of the system before the adsorption, suggesting that this could be a transition configuration leading to a lower energy chemisorbed configuration, as observed for aluminum and silicon surfaces.^{48,49} One can already observe that chains with a larger flexibility, like that in Figure 2i, can more easily accommodate the deformations induced by the oxygen chemisorption, therefore resulting in lower energies.

The donation of a further electron to the remaining partially occupied O₂ π^* orbital leads to a singlet peroxy chemisorbed state, where another C–O bond forms and the O–O bond length further increases to about 1.5 Å (Figure 3c). This chemisorbed reaction is exothermic with an associated energy gain ranging from 0.58 to 1.69 eV, depending on the curvature and flexibility of the carbon chain. The same chemisorbed configurations and similar energies are obtained for triple bonds on polyynic C₈ chains (red symbols in Figure 3 plot). The main difference here is that O₂ can favorably adsorb on two perpendicular planes, corresponding to the two π orbitals of the triple C–C bond. As mentioned above, although the energy gain upon chemisorption depends on the flexibility of the chain, the chemical details of the chemisorption reaction depend on the chemical characteristics of the adsorption site only. As a matter of fact, the involved charge transfer is localized on the oxygen atoms and the two carbon atoms at the adsorption site, the charge on the rest of the carbon atoms not being significantly perturbed by the reaction. As a further evidence, we

obtain the same local minimum geometries on a C₁₀ chain anchored to a periodic acene structure (Figure 2k) and the calculated energies (red triangles in Figure 3) are similar to the energy values obtained for the H-terminated C₈ structures. The energies of analogous configurations on C₉, C₁₂ and C₂₀ chains are reported in the Supporting Information.

Chain cleavage

For both double and triple bonds, the breaking of the O–O bond of the chemisorbed O₂, characterized by the filling of the σ^* antibonding orbital (see Supporting Information), is an exothermic reaction leading to another local energy minimum (Figure 3d). However, while the energy gain ranges between 0.95 and 1.25 eV in the double bond case, it is larger (ranging between 2.17 and 3.07 eV) for triple C–C bonds. The energy minimum configurations described so far describe a possible exothermic reaction path leading to the chemisorption of O₂ at double and triple bonds of cumulenic and polyynic supported chains, and to the consequent rupture of the O–O bond. Analogous configurations were observed during DFT-based molecular dynamics simulations of O₂ adsorption on aluminum and silicon surfaces.^{48,49}

We next investigate whether the breaking of the C–C bond at the adsorption site is an exothermic reaction as in the gas-phase case. Crucially, as visible from the plot of Figure 3, this is true for double C–C bonds but not in general for triple bonds. Our calculations show that the cleavage of the chain at a double C–C bond, resulting in two CO-terminated chain fragments (Figure 3e), is accompanied by an energy gain ranging between 1.38 eV, for the least strained configuration of Figure 2i, and 3.20 eV, for the most strained chain of Figure 2j. A lower value is obtained for the least strained C₁₀ of Figure 2k. However, the rupture of a triple C–C bond is in general an endothermic reaction, unless the chain is sufficiently strained, as in the case of the structures in Figure 2j and Figure 2k, where the C–C bond breaking is accompanied by a 0.24 eV energy gain. This can be understood from the bonding structure of the cleaved chains: While the newly formed C–O double bond is compatible with the bonding structure of a cumulenic chain, it perturbs the ideal single/triple bond alternation of a polyynic structure. However, for sufficiently strained chains, the

release of strain energy can compensate the energy increase due to the perturbation of the bonding structure.

As mentioned before, changing the relative orientation of the terminal CH_2 groups of a cumulenic chain with respect to the ground state orientation³⁵ perturbs the ideal stacking of the π orbitals, introducing a torsional strain and changing the spin state of the system. This is the case of the structure depicted in Figure 2e. As visible from the ELF isosurfaces (Figure 2g), the C–C bonds close to the terminal groups of the chain retain their double bond character whereas the central one does not. Polyynic chains are not affected by this torsional strain but adding a carbon atom to an even-numbered, CH_3 -terminated chain similarly perturbs its single/triple bond alternation (Figure 2f) and the two resulting central bonds are neither single nor triple bonds (Figure 2h). The results for the adsorption and cleavage at these non-ideal bonds are represented as green symbols in Figure 3. Although we were not able to find a stable peroxy configuration in both cases, the superoxy structure is more stable than in the double and triple bond cases. An energy gain of 0.84 eV upon O_2 adsorption is obtained for the structure in Figure 2f. Moreover, both the O–O and C–C cleavage reactions are exothermic, with a larger energy gain for the perturbed cumulenic case.

Reaction kinetics

The energetic analysis just presented allows us to discriminate between possible and impossible reaction sites on supported carbynoid structures but gives no information about the kinetics of the energetically viable reactions. The calculation of reaction barriers for all possible chain configurations is out of the scope of this work. Yet, it is instructive to perform this kind of calculations for some of the structures considered before to investigate the kinetic viability of the proposed adsorption and cleavage reactions. A main difficulty here is that, as in the gas phase, the system can undergo a triplet-to-singlet spin transition during the chemisorption reaction. Following the same approach used for the gas-phase clusters, we avoid spin-flips in the evaluation of the chemisorption energy barriers by constraining the total spin of the system to the doublet state and using an odd

number of terminal H atoms. In order to do so, we add a hydrogen atom to the cumulenic model systems of Figure 2a and Figure 2i. The resulting systems are depicted in Figure 4a,c and the ELF isosurfaces (Figure 4b,d) on the central C–C bond look qualitatively intermediate between those of a double and a triple bond. As the energetics of O₂ chemisorption on double and triple C–C bonds is similar (see Figure 3), we use this bond to measure a typical value for the chemisorption potential energy barrier.

The potential energy barriers along the path leading to the chemisorption of O₂, and to the O–O and C–C cleavage are plotted in Figure 4 for the model systems in Panels a (black line) and c (red line). The minimum energy paths were determined with the Nudged Elastic Band (NEB) method.⁴² In both cases the energy barriers for the chemisorption process are compatible with room temperature oxidation reactions. The barrier leading to the superoxo configuration (Figure 3b) is 0.47 eV and 0.34 eV for the black and red curves, respectively. However, the reaction is exothermic in the second case only. In all cases, the reaction yielding the peroxy configuration (Figure 3c) is exothermic and the associated energy barriers are 0.42 eV and 0.10 eV. Overcoming a small barrier (0.21 eV for the black curve, and a negligible one for the other case) leads to the rupture of the O–O bond. This configuration is however more stable than the fully cleaved one (Figure 3e). Also the triple bonds discussed above show a stable broken O–O adsorption configuration, where sufficient strain restores an energetically favorable configuration with a broken C–C bond. Comparing the black and red curve, one can see that the curvature of the chain helps to stabilize the C–C cleaved doublet chain as well.

However, the two, O–O and C–C, bond breaking reactions leading to the chain's cleavage occur on the singlet potential energy surface and therefore can be calculated using a model system in the singlet spin state. We therefore compare the curves obtained for the doublet case in the configuration of Figure 2i, with analogous cumulenic and polyynic structures. The potential energy curves are depicted in green (cumulene) and blue (polyyne). The behavior of the potential energy during the cleavage reactions of the doublet system is intermediate between the singlet double and triple bond cases. In the case of the exothermic cleavage (cumulenic chain, green curve), the

barriers for the O–O and C–C breaking are 0.29 eV and 0.34 eV, respectively (*i.e.* much lower than the potential energy gained up to that stage of the cleavage process). This indicates that the exothermic cleavage reactions are not limited by the kinetics.

Chain shortening and CO₂ formation

In general, this cleavage reaction is driven by the formation of very strong C–O bonds and has sizeable associated energy gain. This is however smaller than in the gas phase and surely insufficient to cause the detachment of the terminal CO groups, since it is readily dissipated through the substrate. Consequently, we investigate the adsorption of additional O₂ on the CO-terminated supported chains. Our calculations reveal a possible path for their progressive shortening, which proceeds through the chemisorption of O₂ and the subsequent formation of CO₂ as shown in Figure 5a-d, following the same O–O and C–C concerted bond-breaking process discussed above. On both CH₂- and CH₃-terminated C₄O fragments, the O₂ chemisorption yields a peroxo configuration and is exothermic. The adsorption energies are similar in the two cases (1.36 eV and 1.21 eV, *i.e.* in the same energy range as the peroxo state of Figure 3). Similarly, the combined O–O and C–C cleavage produces a CO₂ molecule via the reaction $C_nO + O_2 \longrightarrow C_{n-1}O + CO_2$, which is exothermic with energy gains of 4.72 eV and 4.79 eV. Moreover, on the acene substrate of Figure 2k the above reaction with $n=2-5$ is characterized by a gain in potential energy ranging between 4.10 and 5.88 eV. As long as both the atoms involved in the cleaving C–C bond are *sp*-coordinated, the reaction has an associated potential energy barrier of about 0.6 eV.

The C atom connecting the chain to the surface is either *sp*²- or *sp*³-coordinated. Therefore, we study the energetics of this shortening reaction for the last C–C bond of the chain, where one of the C atoms is a surface atom, using the model systems in Figure 5e and Figure 5f for the *sp*²- and *sp*³-coordinations, respectively. In both cases the $C(s)CO + O_2 \longrightarrow C(s)O + CO_2$ reaction, where *s* labels the C atom belonging to the surface, is exothermic, with a potential energy gain of 4.76 eV (*sp*²) and 4.03 eV (*sp*³). However, while the potential energy barrier for the reaction is about 0.65 eV in the *sp*²-coordination case (Figure 5g-i), we found a minimum of 2.5 eV in

the sp^3 -coordination case. This suggests that the shortening mechanism presented here can lead to different terminations of anchoring surface atoms, depending on the structure and coordination of the terminal sites. For instance, in the model systems considered here, sp^2 -coordinated surface C atoms are O-terminated, while sp^3 -coordinated surface sites could be temporarily terminated by OCO_2 (Figure 5j), as the chemisorption of O_2 in a superoxo configuration is exothermic. The oxidoperoxidocarbonate radical in Figure 5j can be saturated by hydrogen (Figure 5k)⁵⁰ and further chemical reactions in air lead to COO^- or COOH terminations.

Conclusions

In conclusion, we presented a multi-step reaction for the cleavage and shortening of carbynoid structures in presence of O_2 . This reaction was previously hypothesized for the cleavage of cyclic carbon clusters in the gas phase.³² The chemisorption of O_2 molecules on C–C bonds of carbynoid structures triggers the breaking of the O–O and C–C bonds, resulting in the cleavage of the chain and the formation of two O-terminated fragments. Consecutive O_2 -induced C–C bond breaking reactions shorten the O-terminated fragments up to their complete disappearance, producing CO_2 .

Although this shortening mechanism is generally valid for O-terminated chain fragments, because the character of the C–C bond next to the O atom is mainly determined by the C–O bond, the formation of the fragments through O_2 -induced chain cleavage is not. We find that both O_2 chemisorption and C–C cleavage are exothermic and kinetically viable reactions in the case of double bonds of cumulenic chains. While the overall oxidation reaction that leads to the formation of two O-terminated chains is exothermic in all cases, the O_2 chemisorption is not favorable at single bonds of polyynic structures, and C–C cleavage is not exothermic for triple bonds unless the chain is sufficiently strained. These results are compatible with recent works^{17–21} which report the synthesis of polyynic chains that are relatively stable in presence of moisture and oxygen²¹ if terminated by complex end-capping groups.

The scenario proposed here is in agreement with the experimental analysis of Casari *et al.*,²⁹

where the existence of a cleavage process shortening cumulenic and polyynic chains is hypothesized. Their work shows that cumulenic chains are rapidly destroyed upon oxygen exposure, while the degradation of polyynic chains is slower. However, in contrast with the previously mentioned polyynes, that are synthesized in solution, only a small percentage of the polyynic chains survive the exposure to air. A reason for this could be that, in general, carbon chains obtained by cluster deposition or observed in material processes can be expected to be mechanically strained or “non-ideally” terminated. Indeed, the electronic and mechanical properties of the carbynoid structures are strongly influenced by the structure of their terminations³⁴ and by their bending:³³ If displacements of the carbon atoms are allowed by the strain on the chain, the chemisorption, which requires the distortion of the chain structure, is usually easier. Also, as previously mentioned, increasing the bending of supported carbynoid structures (*i.e.* their curvature) facilitates the rupture of the C–C bond at the adsorption site so that even the cleavage of polyynic chains at triple bonds becomes exothermic.

Electronically “non-ideal” cumulenic and polyynic chains were modelled by rotating the terminating groups or adding an additional C atom to the chain, respectively. The model systems investigated here indicate that the O₂-induced cleavage mechanism is exothermic also in these non-ideal cases as long as the C–C bonds are not single bonds. However, these “anomalities” affect the chemisorption configuration and the spin of the system, and might in turn have an effect on the reaction kinetics. For instance, we were not able to find a local minimum with a peroxo configuration in the potential energy surface of some of these structures. Moreover, the perturbed cumulene structure of Figure 2e has still a triplet spin state after O₂ chemisorption and O–O bond breaking, possibly affecting the kinetics of the C–C bond breaking that leads to a singlet spin state.⁴⁵ These aspects deserve a deeper and systematic study since the knowledge of such effects might help developing techniques to stabilize carbynoid structures in presence of oxygen.

Besides revealing details about the oxidation of carbynoid structures, this study casts light on the degradation of carbon chains that spontaneously form during many nanoscale material processes, such as the mechanical polishing of diamond surfaces,¹⁵ the wear of amorphous carbon,³¹

and the growth of amorphous carbon films by chemical vapor deposition¹⁴ or by cluster-beam deposition.²² These structures, whose existence is postulated by atomic-scale simulations or detected experimentally in ultra high vacuum, disappear when exposed to air. The knowledge of the atomic-scale details of the degradation mechanism can lead to predictions on the chemical structure of these carbon substrates. For example, both oxygen- and carboxyl-termination of the sites anchoring the chains to the carbon substrate are possible as a result of the oxygen-induced shortening process. Here, the specific termination is fully determined by the coordination and geometry of the anchoring site.

Acknowledgement

We are grateful to Lucio Colombi Ciacchi for helpful discussions. We acknowledge financial support from BMBF (Grant 03X2512G), BMWi (Grant 0327499A) and from the European Commission (FP7 Marie-Curie Grant 272619 for L. P.). The simulations were carried out at Fraunhofer IWM and NIC Juelich.

Supporting Information Available

Relative energies of linear and cyclic C_n^+ clusters calculated with DFT and compared with other levels of theory. Energetics of the oxygen-induced cleavage reaction for further chain lengths. The evolution of the density of states during the O–O and C–C bond breaking reactions. This material is available free of charge via the Internet at <http://pubs.acs.org/>.

References

- (1) Smith, P. P. K.; Buseck, P. R. *Science* **1982**, *216*, 984.
- (2) Heimann, R. B.; Kleiman, J.; Salansky, N. M. *Nature* **1983**, *306*, 164.
- (3) Whittaker, A. G. *Science* **1985**, *229*, 485.

- (4) Standley, B.; Bao, W.; Zhang, H.; Bruck, J.; Lau, C. N.; Bockrath, M. *Nano Letters* **2008**, *8*, 3345–3349, PMID: 18729415.
- (5) Wang, Y.; Lin, Z.-Z.; Zhang, W.; Zhuang, J.; Ning, X.-J. *Phys. Rev. B* **2009**, *80*, 233403.
- (6) Börrnert, F. et al. *Phys. Rev. B* **2010**, *81*, 085439.
- (7) Meyer, J. C.; Girit, C. O.; Crommie, M. F.; Zettl, A. *Nature* **2008**, *454*, 319–322.
- (8) Chuvilin, A.; Meyer, J. C.; Algara-Siller, G.; Kaiser, U. *New J. Phys.* **2009**, *11*, 083019.
- (9) Muramatsu, H.; Kim, Y. A.; Hayashi, T.; Endo, M.; Terrones, M.; Dresselhaus, M. S. *Small* **2007**, *3*, 788–792.
- (10) Marques, M. A. L.; Troiani, H. E.; Miki-Yoshida, M.; Jose-Yacaman, M.; Rubio, A. *Nano Lett.* **2004**, *4*, 811–815.
- (11) Bogana, M.; Bogana, M.; Ravagnan, L.; Casari, C. S.; Zivelonghi, A.; Baserga, A.; Li Bassi, A.; Bottani, C. E.; Vinati, S.; Salis, E.; Piseri, P.; Barborini, E.; Colombo, L.; Milani, P. *New J. Phys.* **2005**, *7*, 81.
- (12) Yamaguchi, Y.; Colombo, L.; Piseri, P.; Ravagnan, L.; Milani, P. *Phys. Rev. B* **2007**, *76*, 134119.
- (13) Moseler, M.; Gumbsch, P.; Casiraghi, C.; Ferrari, A. C.; Robertson, J. *Science* **2005**, *309*, 1545.
- (14) Ma, T.-B.; Hu, Y.-Z.; Wang, H. *J. Appl. Phys.* **2008**, *104*, 064904.
- (15) Pastewka, L.; Moser, S.; Gumbsch, P.; Moseler, M. *Nature Mater.* **2011**, *10*, 34–38.
- (16) Kastner, J.; Kuzmany, H.; Kavan, L.; Dousek, F. P.; Kuerti, J. *Macromolecules* **1995**, *28*, 344–353.

- (17) Zheng, Q.; Bohling, J. C.; Peters, T. B.; Frisch, A. C.; Hampel, F.; Gladysz, J. A. *Chem. Eur. J.* **2006**, *12*, 6486–6505.
- (18) Bruce, M. I.; Zaitseva, N. N.; Nicholson, B. K.; Skelton, B. W.; White, A. H. *J. Organomet. Chem.* **2008**, *693*, 2887–2897.
- (19) Kim, S. *Angew. Chem. Int. Ed.* **2009**, *48*, 7740–7743.
- (20) Chalifoux, W. A.; McDonald, R.; Ferguson, M. J.; Tykwinski, R. R. *Angew. Chem. Int. Ed.* **2009**, *48*, 7915–7919.
- (21) Chalifoux, W. A.; Tykwinski, R. R. *Nature Chem.* **2010**, *2*, 967.
- (22) Ravagnan, L.; Siviero, F.; Lenardi, C.; Piseri, P.; Barborini, E.; Milani, P.; Casari, C. S.; Li Bassi, A.; Bottani, C. E. *Phys. Rev. Lett.* **2002**, *89*, 285506.
- (23) Hu, A.; Rybachuk, M.; Lu, Q. B.; Duley, W. W. *Appl. Phys. Lett.* **2007**, *91*, 131906.
- (24) Compagnini, G.; D’Urso, L.; Puglisi, O.; Baratta, G. A.; Strazzulla, G. *Carbon* **2009**, *47*, 1605–1612.
- (25) Matsutani, R.; Ozaki, F.; Yamamoto, R.; Sanada, T.; Sanada, Y.; Kojima, K. *Carbon* **2009**, *47*, 1659–1663.
- (26) Jin, C.; Lan, H.; Peng, L.; Suenaga, K.; Iijima, S. *Phys. Rev. Lett.* **2009**, *102*, 205501.
- (27) Zhao, C.; Kitaura, R.; Hara, H.; Isle, S.; Shinohara, H. *J. Phys. Chem. C* **2011**, *115*, 13166–13170.
- (28) Casari, C. S.; Russo, V.; Li Bassi, A.; Bottani, C. E.; Cataldo, F.; Lucotti, A.; Tommasini, M.; Del Zoppo, M.; Castiglioni, C.; Zerbi, G. *Appl. Phys. Lett.* **2007**, *90*, 013111.
- (29) Casari, C. S.; Li Bassi, A.; Ravagnan, L.; Siviero, F.; Lenardi, C.; Piseri, P.; Bongiorno, G.; Bottani, C. E.; Milani, P. *Phys. Rev. B* **2004**, *69*, 075422.

- (30) Milani, A.; Lucotti, A.; Russo, V.; Tommasini, M.; Cataldo, F.; Li Bassi, A.; Casari, C. S. *J. Phys. Chem. C* **2011**, *115*, 12836–12843.
- (31) Moras, G.; Pastewka, L.; Gumbsch, P.; Moseler, M. *Tribol. Lett.* **2011**, *44*, 355–365.
- (32) Sowa, M. B.; Anderson, S. L. *J. Chem. Phys.* **1992**, *97*, 8164.
- (33) Hu, Y. H. *J. Phys. Chem. C* **2011**, *115*, 1843–1850.
- (34) Ravagnan, L.; Manini, N.; Cinquanta, E.; Onida, G.; Sangalli, D.; Motta, C.; Devetta, M.; Bordoni, A.; Piseri, P.; Milani, P. *Phys. Rev. Lett.* **2009**, *102*, 245502.
- (35) Gu, X.; Kaiser, R. I.; Mebel, A. M. *ChemPhysChem* **2008**, *9*, 350–369.
- (36) Mortensen, J. J.; Hansen, L. B.; Jacobsen, K. W. *Phys. Rev. B* **2005**, *71*, 035109.
- (37) Enkovaara, J. et al. *J. Phys.: Condens. Matter* **2010**, *22*, 253202.
- (38) Perdew, J. P.; Burke, K.; Ernzerhof, M. *Phys. Rev. Lett.* **1996**, *77*, 3865–3868.
- (39) Tao, J.; Perdew, J. P.; Staroverov, V. N.; Scuseria, G. E. *Phys. Rev. Lett.* **2003**, *91*, 146401.
- (40) Bitzek, E.; Koskinen, P.; Gähler, F.; Moseler, M.; Gumbsch, P. *Phys. Rev. Lett.* **2006**, *97*, 170201.
- (41) Tang, W.; Sanville, E.; Henkelman, G. *J. Phys.: Condens. Matter* **2009**, *21*, 084204.
- (42) Henkelman, G.; Jónsson, H. *J. Chem. Phys.* **2000**, *113*, 9978.
- (43) Baer, T.; Hase, W. L. *Unimolecular Reaction Dynamics*; Oxford University Press: New York, 1996.
- (44) Giuffreda, M. G.; Deleuze, M. S.; Franois, J. P. *J. Phys. Chem. A* **1999**, *103*, 5137–5151.
- (45) Burgert, R.; Schnöckel, H.; Grubisic, A.; Li, X.; Stokes, S. T.; Bowen, K. H.; Ganteför, G. F.; Kiran, B.; Jena, P. *Science* **2008**, *319*, 438–442.

- (46) Becke, A. D.; Edgecombe, K. E. *J. Chem. Phys.* **1990**, *92*, 5397.
- (47) Savin, A.; Nesper, R.; Wengert, S.; Fässler, T. F. *Angew. Chem. Int. Ed.* **1997**, *36*, 1808–1832.
- (48) Colombi Ciacchi, L.; Payne, M. C. *Phys. Rev. Lett.* **2004**, *92*, 176104.
- (49) Colombi Ciacchi, L.; Payne, M. C. *Phys. Rev. Lett.* **2005**, *95*, 196101.
- (50) Ingold, K. *Chem. Rev.* **1961**, *61*, 563.

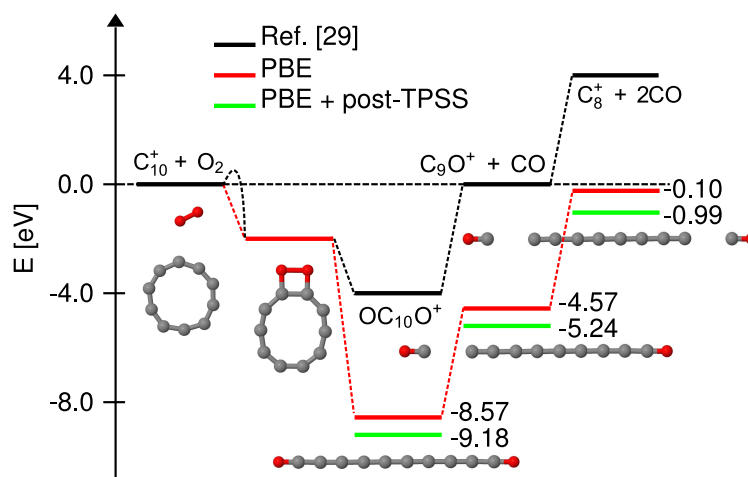


Figure 1: Schematic representation of the potential energy landscape for the O_2 -induced cleavage of the C_{10}^+ cluster as estimated by Sowa *et al.*³² (black line) and as calculated in this work (red and green lines). The insets show the system configurations corresponding to each potential energy local minimum represented in the plot.

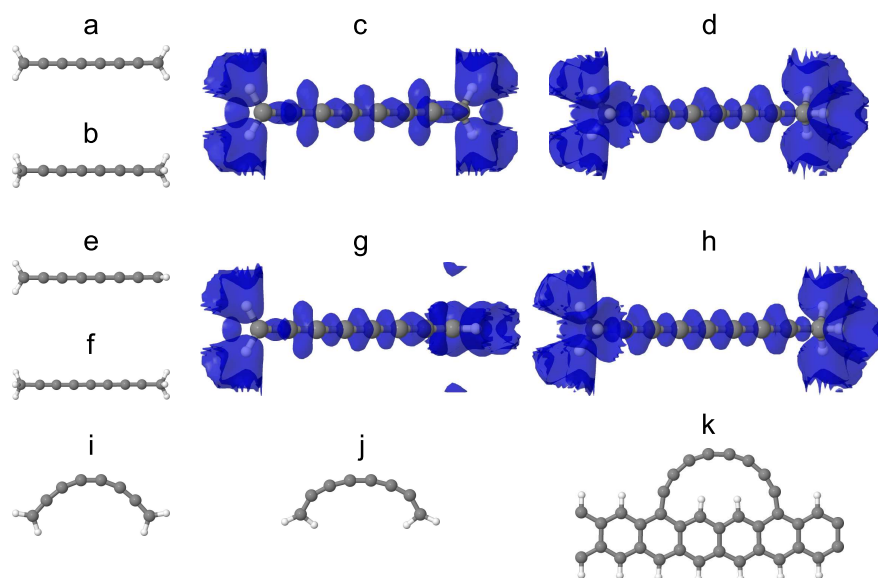


Figure 2: Model systems of supported carbynoid structures: (a) straight cumulenic C_8 ; (b) straight polyynic C_8 (the two different bonding structures are visible from the Electron Localization Function (ELF) isosurfaces in Panels c and d); (e) system of Panel a perturbed by rotating one of the terminal CH_2 groups by 90° ; (f) system of Panel b perturbed by adding one carbon atom to the chain; (g,h) ELF isosurfaces for the structures in Panels e and f; (i,j) curved structures with different curvatures imposed by varying the positions of the terminal H atoms; (k) C_{10} chain supported by a periodic acene structure.

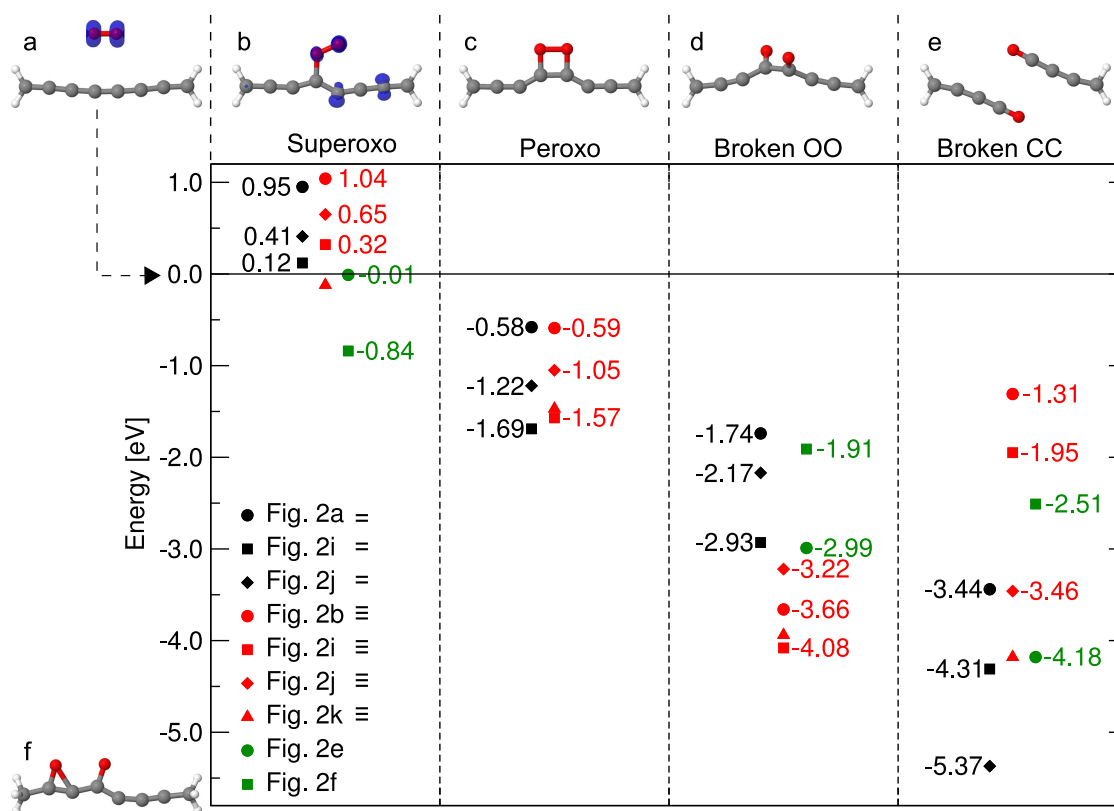


Figure 3: Potential energy minima along a possible reaction path (Panels a-e) leading to the chemisorption of O₂ on supported carbynioid structure and to the cleavage of the latter. The three sets of colors refer to chemisorption at double (black), triple (red) and "hybrid" (green) C–C bonds. The latter are obtained by perturbing the ideal cumulenic or polyynic structure through the rotation of a terminal CH₂ group or the addition of one C atom (see text for details). The legend refers to the structures shown in Figure 2, while the = and ≡ symbols refer to double and triple C–C bonds, respectively, as adsorption sites. The reaction path includes the configurations depicted in Panels a-e (here a straight cumulenic chain is used as example): (a) non-adsorbed triplet O₂ (the blue isosurfaces represent the spin polarization density); (b) superoxo chemisorbed state; (c) peroxy spin-paired chemisorbed state; (d) broken O–O bond; (e) cleaved chain. Panel f shows the configuration obtained upon O₂ chemisorption at a single C–C bond.

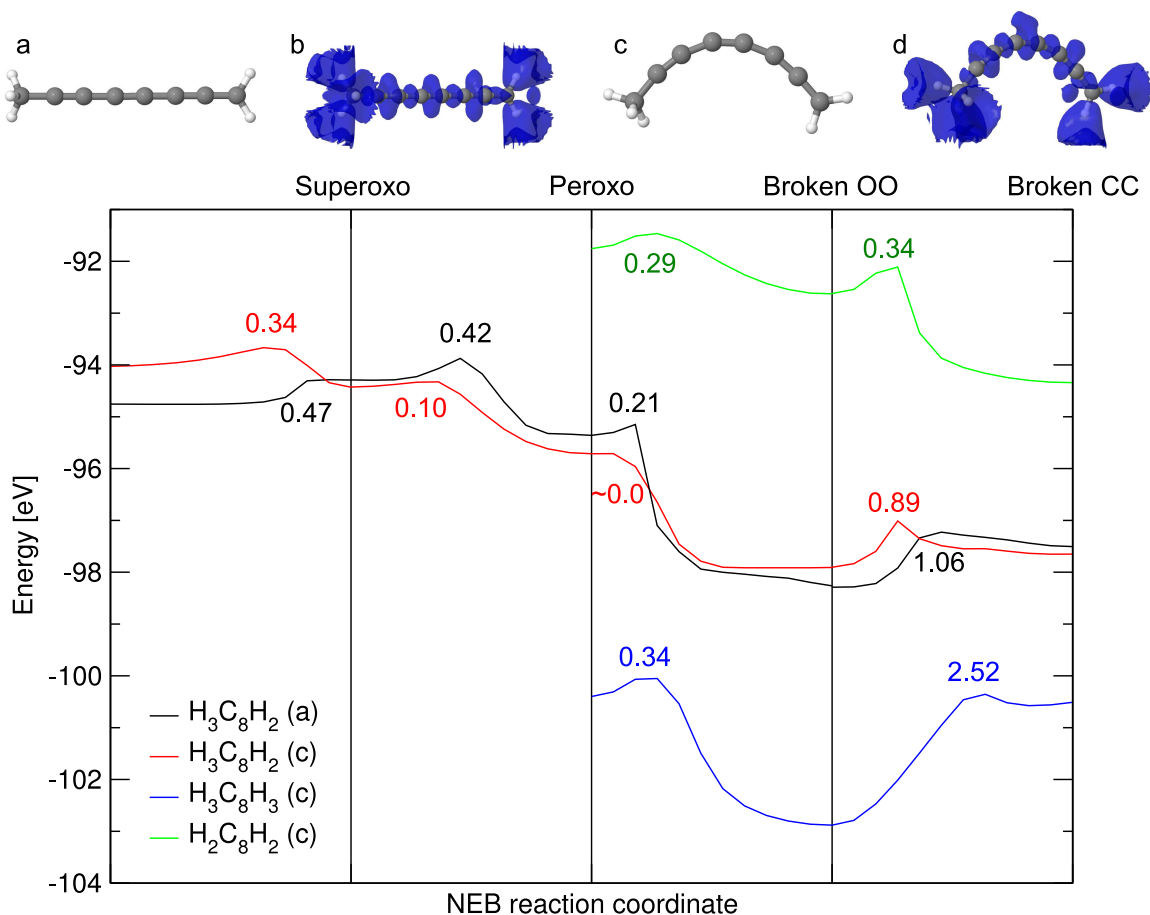


Figure 4: Potential energy barriers calculated with the NEB method for the O_2 adsorption on a supported carbon chain, and the consequent cleavage of O–O and C–C bonds. The black and red curves refer to the model systems of Panels a and c, respectively. These model systems are similar to those in Figure 2a and i, but a hydrogen atom has been added to obtain a doublet spin state. The corresponding ELF isosurfaces for $\text{ELF}=0.8$ are plotted in Panels b and d. The blue and green curves represent the potential energy surface for the O–O and C–C bond breaking reaction in the case of a polyynic and a cumulenic chain, having the structure of Figure 2i. The numbers reported on the plot are the values of the energy barriers in electronvolts.

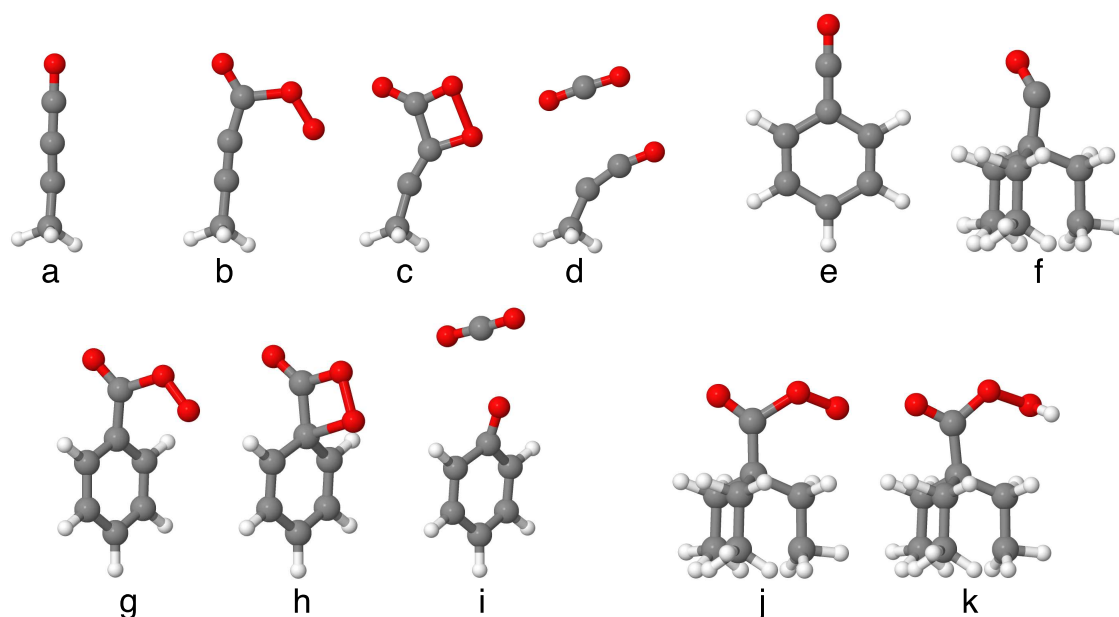


Figure 5: O_2 -induced cleavage yields shortening of the CO-terminated chains and formation of CO_2 (a-d). The C atom connecting the chain to the underlying C surface, can be either sp^2 - (e) or sp^3 -coordinated (f). Fixing the positions of the three lower C atoms in panels e and f and of their H terminations, we find that a further concerted O–O and C–C bond breaking is possible in the sp^2 case (g-i). The same reaction is not kinetically viable for the sp^3 -coordination case instead (j), leading to temporary OCO_2H termination (k).

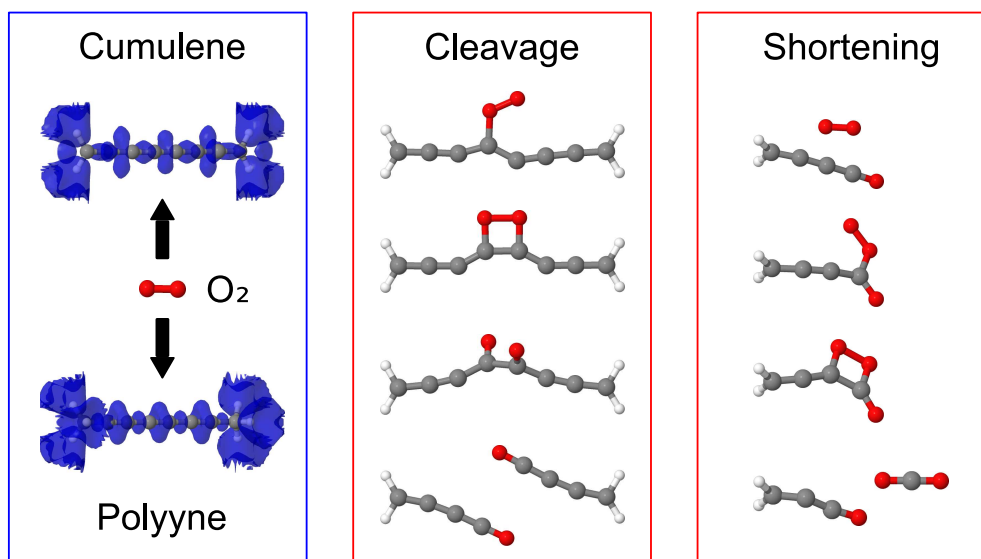


Figure 6: Table of Contents Graphic